

Simulation of the Acoustic Environment for the Manufacture of Graded Porosity Materials by Sonication

Carmen Torres-Sánchez* and Jonathan R. Corney

Department of Design, Manufacture and Engineering Management (DMEM),
University of Strathclyde

*Corresponding author: James Weir Building, 75 Montrose Street, Glasgow, G1 1XJ, United Kingdom,
email: carmen.torres@strath.ac.uk

Abstract:

Many materials require functionally graded cellular microstructures whose porosity is engineered to meet specific requirements of diverse applications (e.g. polymers and/or ceramics that mimic biological material such as soft tissue and bone). It has been shown in previous work that the bubble growth rate of a polymeric foam can be influenced by the surrounding acoustic environment and, once solidified, produce a solid of graded porosity. Motivated by the desire to create a flexible process for engineering graded foams this work investigated how a COMSOL™ model was developed for assessing the acoustic environment that a foaming melt was subjected to. The COMSOL™ model has demonstrated good correspondence with the experimental results. The ability to predict the interactions of ultrasound with the polymeric materials undergoing foaming will allow this phenomenon to be exploited further in the manufacture of porous materials with engineered cell sizes and distributions.

Keywords: polymeric foam, ultrasound, acoustic pressure, porosity gradation, acoustic impedance.

1. Introduction

Unique functional requirements can be obtained when a material's structure or composition is varied within a component. A prime example of this is a variety of bio-materials that require functionally graded cellular microstructures whose porosity is engineered in order create unique transport conduits or reaction surfaces. Numerous applications have demonstrated the success of this approach in areas ranging from biomaterial science through to structural engineering (e.g. polymer and/or ceramics that mimic biological material such as soft tissue and bone; structural polymers and foams with specific mechanical, thermal

properties, etc). Polymeric foams are a particular example of graded cellular microstructures and the authors' earlier work [1-3] has shown that a flexible process for engineering graded foams can be enabled by the application of ultrasound during specific stages of the polymeric foaming process producing similar structures to biological materials such as bone or plant stems (Figure 1a and b).

In that work it was found that the rate of bubble growth in a polymeric melt undergoing foaming could be influenced by the ultrasonic environment (i.e. sound pressure, frequency and exposure time). Consequently, once the foam solidified, the final porosity distribution within the solid, foamed material reflected these sonication conditions. Results showed that bubble enlargement was proportional to the

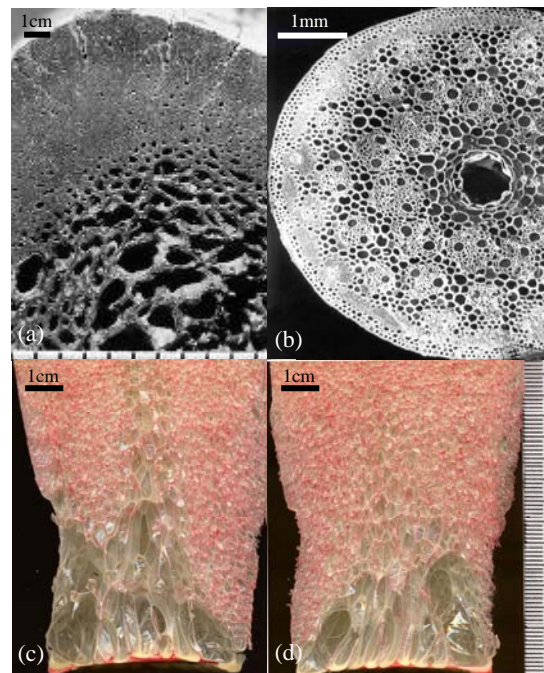


Figure 1: Cross-sections (a) Bone, (b) Bamboo stem – obtained by CPD–, (c) Polymeric foam irradiated at 20kHz and 26000Pa, 3.70cm from probe, (d) Polymeric foam irradiated at 30kHz and 8900Pa, 4.90cm

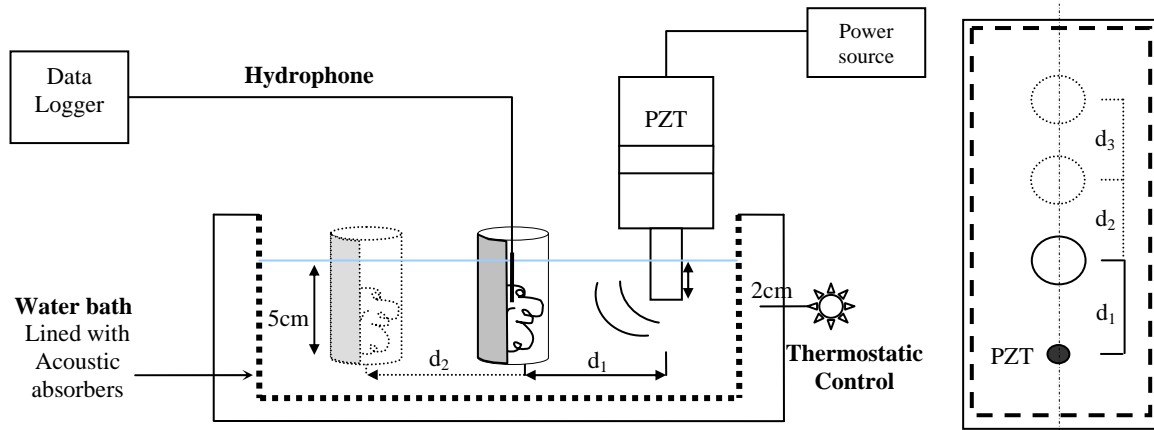


Figure 2: Schematic of the experimental rig

sound pressure when this was above a lower threshold value (below which there was no effect on the cellular structure), and below than an upper threshold (above which cavitation occurred causing an implosion of bubbles). Between these limits, bubbles exhibited a resonant behavior causing them to grow. The authors' thesis was that the amount of growth would correlate with the strength of the acoustic signal within the bath. However, the acoustic environment inside a container was very complex, with numerous peaks and troughs.

Once the ultrasonic effect on the bubbles' size and position was proven experimentally, the exploitation of this phenomenon for the engineering of cellular structures with 'ad-hoc' morphology required a simulation tool that would permit an acoustic environment to be created that matches the materials' functional requirements.

COMSOL™ was chosen to simulate the interactions of ultrasound with a foaming melt that solidifies to produce a solid material with a graded porosity because of its capacity to couple the acoustic pressure effect on the geometry of a foaming structure.

This paper is divided into the following sections: Methodology, where a description of both the experimental rig tested and the COMSOL™ Multiphysics model used for this application is presented. Section 3 contains a summary of the results obtained and the discussion is found in section 4. Finally, the main conclusions are drawn in section 5 and future work with the COMSOL™ model presented.

2. Methodology

2.1 Experimental rig

To investigate the foam sonication phenomenon, a plastic container holding the initial liquid mixture of monomers was immersed in a water bath, which acted as a coupling agent. Once the foaming reaction was started (i.e. after the addition of a catalyst) the ultrasound irradiated the bath (Figure 2). The control of the energy irradiated into the foaming samples was proven to be vital as it determined the foam's cellular structure and pore size distribution.

2.2 The COMSOL™ model

A COMSOL™ model was developed for assessing the acoustic environment that the foaming samples were subjected to when immersed in the water bath. The simulation had to accurately model the effects of both acoustic reflections and the environment inside the container holding the expanding foam. It has proven to be a robust technique for the purpose of studying different irradiation scenarios and, has helped establish how the parameters of ultrasound exposure (i.e. frequency and acoustic pressure) influence the volume and distribution of pores within the final polyurethane matrix.

For the calculation of the acoustic pressure distribution in the water bath, the general wave equation was used. In this case, as the coupling agent is water, the shear stress is neglected, and the wave propagation assumed to be linear. Therefore, the wave equation is expressed in terms of pressure (p), density of the fluid (ρ_0) and speed of sound (c) as:

$$\frac{1}{\rho_0 \cdot c^2} \cdot \frac{\partial^2 p}{\partial t^2} + \nabla \left(\frac{-1}{\rho_0} \cdot \nabla p \right) = 0 \quad (1)$$

The solving option for the pressure was set to time harmonic and, as the pressure variation in time is $p=p_0 \cdot e^{i(\omega t)}$, the wave equation for acoustic waves reduces to the Helmholtz equation, where the angular frequency ($\omega=2\pi f$) is introduced as another variable:

$$\nabla \left(\frac{-1}{\rho_0} \cdot \nabla p \right) - \frac{\omega^2 \cdot p}{\rho_0 \cdot c^2} = 0 \quad (2)$$

The boundary conditions for the water bath walls (which were physically modified to minimize reflections and refractions) and the container material were adjusted so that the model would match the experimental measurements of the acoustic environment previously recorded with hydrophones on the rig (Figure 3).

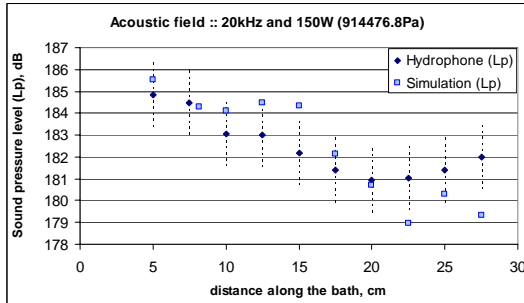


Figure 3: Sound pressure distribution in the yz plane for the modeled scenario and the experimental rig

The discrepancies between measured and simulated results for the sound pressure levels found in the middle and far right of the bath may be due to a variation in the acoustic characterization of the water bath walls (i.e. the acoustic damping was not uniformly applied on the bath walls).

Following an analysis of the sensitivity of the modeled rig [2], the following parameters were adopted for the bath simulation: the water bath walls were set at an impedance corresponding to that of the steel ($Z=45.6$ MRayl) and the water/air interface was simulated as a ‘hard’ wall (i.e. 100% reflective boundary). The radiation condition for the ultrasonic probe was set to

‘cylindrical’ at each of the values required for each individual simulation.

Scalar variables: The pressure reference for the model was set at $20 \cdot 10^{-6}$ Pa for all the simulations and the excitation frequency was 20, 25 or 30 kHz, depending on the simulation series.

Mesh generation: In order to perform the finite element analysis, the domain (i.e. water bath) had to be decomposed into tetrahedrons. This decomposition was automatically achieved by using the available grid generation tools, which discretized the domain using the quadratic Lagrange elements. For the standard model used in this study, the number of tetrahedral elements was set to 6030, which left 1284 mesh points and 8960 degrees of freedom to solve.

Solver settings: time stepping. The model was tested in order to identify the necessary time frame to reach steady state in the simulated conditions. For the water bath simulation model, it was set to 10s. The time stepping for the solving protocol was set to 0.5s and the relative tolerance (i.e. error for the time stepping) was 0.01s. For solving the containers simulation model, the method was set to 1s for the steady state, with a 0.1s stepping and a tolerance of 0.01s.

The COMSOL™ model has demonstrated good correspondence with the experimental results as far as the geometry and nature of the bath and containers are concerned. Having validated the model against physical data, the COMSOL™ model allowed the characterization (i.e. subdomain description and boundary conditions) of the acoustic field *only* within the early and final stages of the irradiated foaming melt. Although the acoustic properties of the initial liquid melt and final solid foam have been described in literature [4- 5], direct measurement is very difficult. Furthermore, the acoustic impedance of the melt changed continuously during the foaming process, which makes the simulation of the acoustic field within the melt undergoing foaming very difficult.

During foam cross-linking, the irradiated medium was a mixture of water, carbon dioxide and polyurethane foam. Therefore, the acoustic impedance was expected to change from an initial value similar to water ($Z_{\text{water}}=1.48$ MRayl) at initial stages of the polymerization reaction, through a resin acoustic impedance (e.g. $Z_{\text{resin}}=1.5-1.8$ MRayl) [6] when the viscosity was high, evolving finally towards a typical acoustic

impedance value in the range of the porous materials (e.g. 7.4-10MRayl) [5] or compact bone (e.g. 9.3MRayl for a density of 1930kg/m³) [7] when the foam was fully cured and dry. For the purpose of the irradiated foam in the simulated bath, the working acoustic impedances that were used corresponded to the water ($Z=1.48\text{MRayl}$; density 1000kg/m³, longitudinal sound velocity $c_s = 1480\text{m/s}$) and to typical cortical bone ($Z_{\text{cort bone}} = 2.6\text{MRayl}$ for a density of 1630kg/m³, $c_s = 1550\text{m/s}$) [8], which matched the expected density of the foam at those stages in the reaction.

3. Results

The data obtained by using the extreme scenarios (i.e. liquid and solid) to represent the acoustic energy levels within the vessel, have already allowed the comparison between the acoustic environment in the foam and the porosity of the corresponding sample cross-section with promising results.

Figure 4 presents a water bath that has a vessel immersed at 4.90cm distance from the probe with the sonotrode irradiating at 30kHz and 8900Pa in a ‘cylindrical’ soundwave shape.

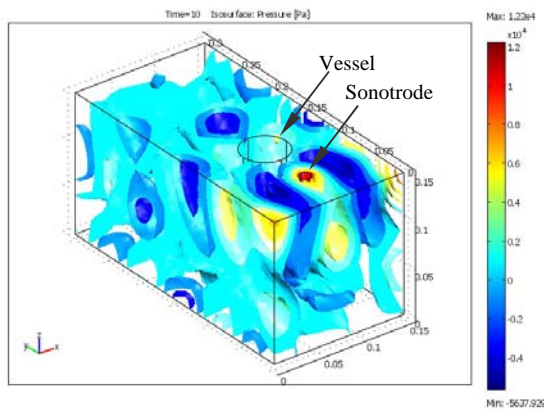


Figure 4: Acoustic field in the water bath with an immersed vessel at 4.90cm from the probe

In order to couple the acoustic field in the water bath to that ‘seen’ by the polymeric foams inside of the containers, the boundary conditions for the vessels must be set (i.e. the acoustic impedance of the polypropylene container). On the outer perimeter of the container, an incident cylindrical wave was specified to represent an

incoming sound wave with the same characteristics given the signal travelling across the water bath for a given distance from the probe.

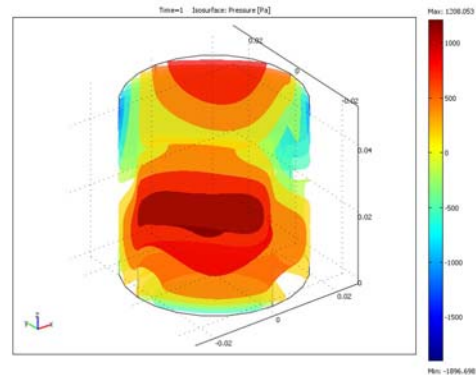


Figure 5: Modeled vessel at 4.90cm from probe showing the acoustic field when irradiated while immersed in the water bath

For solving the model presented in Figure 5, the simulator generated a grid with 13571 elements. The method solved for 19928 degrees of freedom in an averaged solution time of 509.453s. The cross-section presented in Figure 6 shows the sound pressure levels extracted from the vessel in Figure 5 using a vertical plane aligned to the acoustic wave that is received by the containers immersed in the water bath.

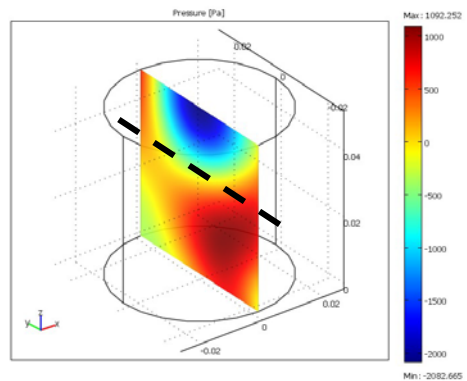


Figure 6: Cross-section (plane) in vessel at 4.90cm from probe

The data provided by Figure 6 was used to establish a comparison between final porosity in the physical foam sample and the acoustic magnitude that the foam had been subjected to during its formation in the water bath: A plane was extracted across the bath in the x and y

directions, using the same z coordinate (i.e. aligned to the sonotrode's tip plane). These lines (dotted for $Z=1.48\text{MRayl}$, the acoustic impedance of a liquid, i.e. the initial content of the vessel, in the early stages of the chemical reaction, can be approximated to liquid water; and dash-and-dotted line for $Z=2.6\text{MRayl}$, the impedance of cortical bone, to represent the final nature of the porous solid foam) were plotted along with the porosity values measured directly on the foam cross-section (Figure 1d) using an image processing application, the 'Topoporosity' tool, that mapped areas of equal porosity value assigning them a value between 0 and 160 to represent the porosity distribution [2-3] (e.g. 160 value, very high porosity; 20 value, very high density). This scale appears on the OY axis in Figure 7.

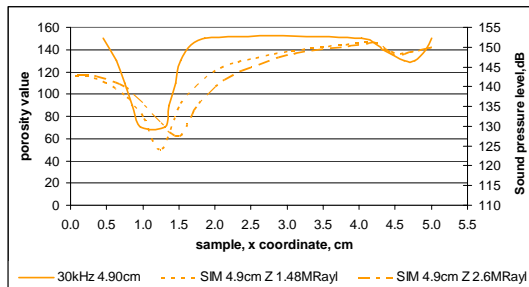


Figure 7: Comparison of porosity (experimental) vs sound pressure distribution (simulation) for the irradiated foam ($Z=1.48\text{MRayl}$ liquid; $Z=2.6\text{MRayl}$ porous solid)

4. Discussion

The simulations performed with the COMSOL™ model for the water bath and the immersed vessels when irradiated with the ultrasound have been verified with the experimental measurements. The high correlation found in the comparison between modeled and experimental results allows further study on the interaction of energy levels in the foaming melt and its final porosity distribution for a fine tailoring of its cellular structure and, one day, the design of artifacts that could mimic natural micro-architectures.

In the current model, the acoustic impedance of the melt has been approximated to values on its initiating and finishing states with very different acoustic characteristics (liquid at an initial stage, and porous solid at a final stage).

Although the bulk porosity (defined as the ratio of void to volume-mass), remained approximately the same from the 'gelation' point (i.e. when the bubbles' walls lock their positions in the matrix) onwards until fully cross-linking of the polymer, the local porosity and, therefore, the acoustic impedance, varied continuously. The acoustic impedance of a viscous fluid is a function of the density of the fluid, its viscosity and the circular frequency ($\omega=2\pi f$) of the ultrasonic wave [9], in the same way that the acoustic impedance of a solid is the resultant value of the product of the solid density and the longitudinal sound velocity.

Following this principle, the incorporation of varying acoustic properties with time for the foaming melt is a crucial next step for a more accurate model that can represent the energy at each point within the growth of the sample. The authors believe this capability would allow a close correspondence to be established between the acoustic pressure and pore architecture.

5. Conclusions and Future work

A COMSOL™ model has been used to simulate the acoustic environment to which polymeric melts, undergoing foaming, were subjected. Initial results of simplified scenarios have proven good correlation with the experimental data. This allows a better understanding of how the manipulation of the acoustic field applied to the melt can control and tailor the bubbles, then pores, to a desired position and size. For example, Figure 8 shows how the acoustic soundwave pattern varies with the position of the vessel inside the bath. The porosity gradation created in the foam at these locations will reflect this sinusoidal energy distribution.

Current work is focused on the definition of acoustic properties which vary with time (i.e. provoked by physical properties such as viscosity) in the foaming melt. Hopefully this will allow a better correlation between the ultrasonic energy and porosity values in the sonicated samples.

Further investigation involves different coupling agents for the water bath and multiple sonotrodes with the intention of a fine control of the acoustic environment for the manufacture of graded porosity materials by sonication.

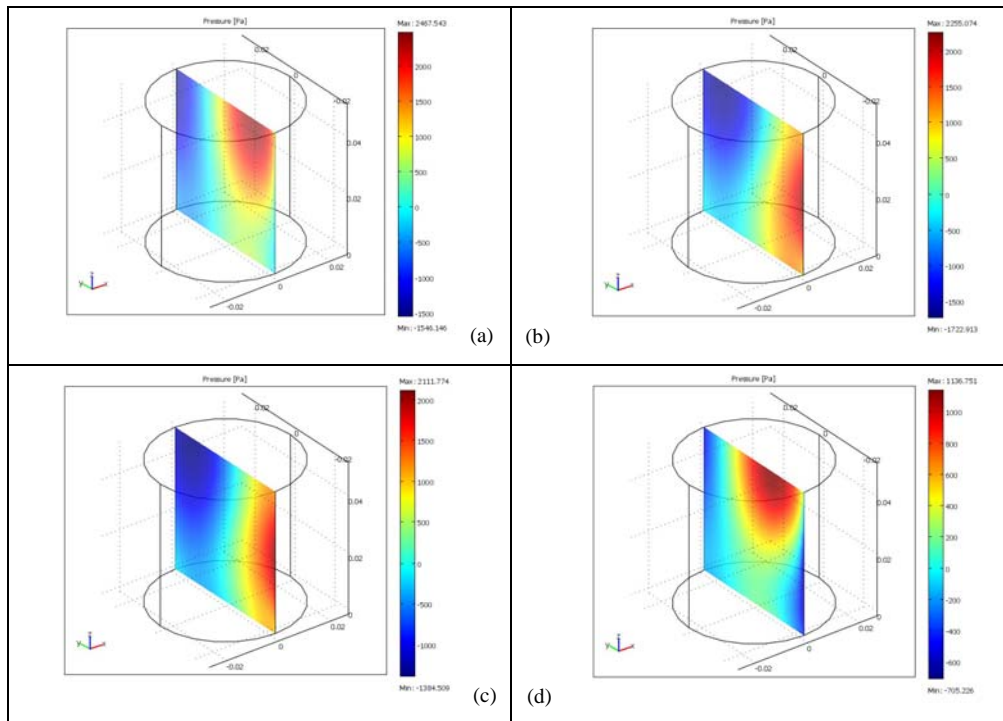


Figure 8: Sinusoidal sound pattern on the foams irradiated at different distances at 20kHz and 18,000Pa: (a) 3.70cm; (b) 7.40cm; (c) 8.60cm; (d) 11.10cm from the sonotrode

The phenomenon discovered in this work offers the prospect of a manufacturing process that can adjust the cellular geometry of foam and hence ensure that the resulting characteristics of the heterogeneous material match the functional requirements.

6. Acknowledgements

The authors would like to thank Dr. A. MacRae from the University of Calgary, Canada, for Figure 1(a) and Quorum Technologies Ltd. for Figure 1(b).

7. References

1. Torres-Sánchez, C. and Corney, J. Effects of ultrasound on polymeric foam porosity, *Ultrasonics Sonochemistry*, **15**, p. 408-415, (2008).
2. Torres-Sánchez, C. *Generation of heterogeneous cellular structures by sonication*. Ph.D. thesis, Edinburgh (UK): Heriot-Watt University (2008)
3. Torres-Sánchez, C. and Corney, J. Towards functionally graded cellular microstructures.

ASME Conference on Smart Materials, Adaptive Structures and Intelligent Systems, Ellicott City, Maryland, USA, SMASIS-414, (2008)

4. Blitz, J. *Fundamentals of ultrasonics*. London: Butterworths & Co. Ltd publishers (1967).

5. Cheeke, J. D. N. *Fundamentals and applications of ultrasonic waves*: CRC publisher. (2002).

6. Albers, V. M. *Underwater Acoustics. Handbook II*: The Pennsylvania State University Press (1965).

7. Raum, K., Cleveland, R. O., Peyrin, F. and Laugier, P. Derivation of elastic stiffness from site-matched mineral density and acoustic impedance maps, *Physics in Medicine and Biology*, **51**, p. 747-758, (2006).

8. Yoshizawa, M., Ushioda, H. and Moriya, T. Development of a bone-mimicking phantom and measurement of its acoustic impedance by the interference method. *IEEE Ultrasonics Symposium*, 1769-1772, (2004)

9. Balasubramaniam, K. and Sethuraman, S. Ultrasonic interferometric sensor for rheological changes of fluids, *Review of Scientific Instruments*, **77**, p. 084902-084908, (2006).